Original Article

Analysis of microRNA expression profiles in porcine PBMCs after LPS stimulation

Jing Zhang[1], Xin Xu[1], Xingfa Huang[2], Huiling Zhu[1],
Hongbo Chen[1], Wenjun Wang[2],* and Yulan Liu[1],* (iD)

Abstract

In the present study, we used microRNA (miRNA) sequencing to discover and explore the expression profiles of known and novel miRNAs in 1000 ng/ml LPS stimulated for 8 h vis-à-vis non-stimulated (i.e. control) PBMCs isolated from the blood of healthy pigs. A total of 291 known miRNAs were bio-computationally identified in porcine PBMCs, and 228 novel miRNAs (not enlisted in the swine mirBase) were identified. Among these miRNAs, ssc-miR-148a-3p, ssc-let-7g, ssc-let-7f, 3_8760, ssc-miR-26a, ssc-miR-451, ssc-miR-21, ssc-miR-30d, ssc-miR-99a and ssc-miR-103 were the top 10 most abundant miRNAs in porcine PBMCs. Through miRNA differential analysis combined with quantitative PCR, we found the expressions of ssc-miR-122, ssc-miR-129b, ssc-miR-17-5p and ssc-miR-152 were significantly changed in porcine PBMCs after LPS stimulation. Furthermore, targets prediction and function analysis indicated a significant enrichment in gene ontology functional categories related to diseases, immunity and inflammation. In conclusion, this study on profiling of miRNAs expressed in LPS-stimulated PBMCs provides an important reference point for future studies on regulatory roles of miRNAs in porcine immune system.

Introduction

In swine production, Gram-negative bacterial infection is one of the most important causes of severe inflammation, which may result in economic losses due to mortality, morbidity and decreased growth rate.[1,2] Endotoxin/LPS, hosted in the outer membrane of Gram-negative bacteria, is a potent activator of the innate immune system.[3] LPS induces macrophage/monocyte activation and pro-inflammatory cytokine (TNF-α, IL-1β and IL-6) production by activating TLR4 signalling.[4] The TLR4/MyD88/NF-κB pathway and the TLR4/TRIF-NLRP3 inflammasome axis are key regulators involved in inflammatory processes.[5,6] However, considering the complexity in the LPS-induced inflammatory response, other levels of regulation may also be involved.

MicroRNAs (miRNAs) represent a class of small non-coding RNAs (17–25 nt) that regulate gene expression through translational inhibition or transcript degradation.[7] Recent studies have shown that miRNAs play a key regulatory role in inflammation. For example, miR-223 reduced LPS-induced inflammation and suppressed the NLRP3 inflammasome and TLR4/NF-κB signalling pathway via targeting rho-related GTP-binding protein RhoB (RHOB).[8] MiR-9 increased LPS-induced inflammatory response of macrophages by targeting silent information regulator 1 (SIRT1).[9]

[1]Hubei Key Laboratory of Animal Nutrition and Feed Science, Hubei Collaborative Innovation Center for Animal Nutrition and Feed Safety, Wuhan Polytechnic University, PR China
[2]Hubei Provincial Key Laboratory for Protection and Application of Special Plants in Wuling Area of China, South-Central University for Nationalities, PR China

*These authors contributed equally to this work.

Corresponding authors:
Yulan Liu, Hubei Key Laboratory of Animal Nutrition and Feed Science, Hubei Collaborative Innovation Center for Animal Nutrition and Feed Safety, Wuhan Polytechnic University, Wuhan 430023, PR China.
Email: yulanflower@126.com
Wenjun Wang, Hubei Provincial Key Laboratory for Protection and Application of Special Plants in Wuling Area of China, Wuhan 430074, PR China.
Email: hustwsir@126.com

Moreover, a number of miRNAs regulate elements of the TLR-signalling cascade or target cytokines directly. MiR-146b directly targets IL-1 receptor-associated kinase 1 (IRAK1) and TNF receptor-associated factor 6 (TRAF6), key adaptor proteins of the TLR4/NF-κB signalling cascade, resulting in inhibition of NF-κB activation and inflammatory cytokine production.[10] MiR-322 inhibits inflammatory cytokine expression in LPS-stimulated murine macrophages by targeting NF-κB1.[11] MiR-93-3p alleviates LPS-induced inflammation by inhibiting TLR4.[12] MiR-27a regulates the inflammatory response of macrophages by targeting IL-10, a potent anti-inflammatory cytokine.[13] However, miR-155 and miR-125b can target the 3′ untranslated region of TNF-α mRNA directly.[14]

Considering the role of miRNAs in the innate immune response, the present study was designed to discover and explore the miRNA profile of porcine PBMCs in response to LPS. To date, miRNA expression in the LPS-induced inflammation in porcine blood cells has not been well characterised. This analysis of miRNA expression in porcine PBMCs challenged with LPS contributes significantly to the current knowledge of miRNAs playing roles in bacterial infection disease pathogenesis.

Materials and methods

Cell isolation, culture and stimulation

The PBMCs from the Duroc×Large White×Landrace (DLW) crossbred piglets (∼15 kg, ∼8 wk old) were isolated by Ficoll-Hypaque density gradient centrifugation at room temperature (25°C). Briefly, heparinised blood was layered on an equal volume of D-Han's solution (pH 7.2), and then an equal volume of Ficoll-Hypaque medium was added in a conical centrifuge tube. The suspension was centrifuged at 472 g for 30 min at room temperature. The PBMC layer was collected and washed three times with D-Han's solution. The PBMCs were cultured in RPMI 1640 medium (Gibco, Scoresby, Australia) supplemented with 10% heat-inactivated FBS (Gibco), 2 mmol/l L-glutamine, 100 IU/ml penicillin and streptomycin (Gibco) at 37°C under 5% CO_2. LPS (*Escherichia coli* serotype 026:B6, Sigma–Aldrich, St Louis, MO) was dissolved (10 μg/ml) in saline solution. PBMCs were cultured at a concentration of 1×10^7/ml per well of a six-well plate. PBMCs were treated with LPS (the final concentration was 1 μg/ml) for 8 h. Cells were further centrifuged for 10 min at 3500 g and harvested for RNA extraction.

Quantitative RT-PCR

Total RNA was isolated from cell samples using Trizol (Invitrogen, Carlsbad, CA) according to the manufacturer's protocol. Expression of TNF-α, IL-1β and IL-6 mRNA was analysed using the Applied Biosystems 7500 Real-Time PCR system (Applied Biosystems, Foster City, CA). cDNA synthesis and quantitative RT-qPCR were carried out as previously described.[15] GAPDH was used as an internal normalisation control. Sequences of specific primers are shown in Supplemental Table S1. miRNA expression was analysed using a Hairpin-it™ miRNA qPCR Quantitation Kit (GenePharma, Shanghai, PR China) and the Applied Biosystems 7500 Real-Time PCR system according to the manufacturer. U6 was used as a normalisation gene. All data were analysed using the $2^{-\Delta\Delta CT}$ method.[16]

Cytokine TNF-α and IL-1β measurements

The concentrations of TNF-α and IL-1β in supernatants of PBMCs were measured using commercially available porcine ELISA kits (R&D Systems, Inc., Minneapolis, MN) according to the manufacturer's instructions.

Small-RNA library construction and deep sequencing

The RNA samples from LPS-stimulated and unstimulated PBMCs of three pigs were used to create three experimental small RNA libraries and three control libraries for biological replicates. For each small RNA library construction, 1 μg total RNA was ligated to a 5′ and a 3′ adapter sequentially according to the protocol (NEBNext® Multiplex Small RNA Library Prep Set for Illumina). Briefly, 1 μg RNA was mixed with 1 μl 3′ SR adaptor and added nuclease-free water up to 7 μl total volume. Then, the mix was incubated in a preheated thermal cycler for 2 min at 70°C. The tube was transferred to ice, and the following components were added: 10 μl 3′ ligation reaction buffer (2×) mix and 3 μl of 3′ ligation enzyme mix. The mix (total volume 20 μl) was then incubated for 1 h at 25°C in a thermal cycler. Next, 4.5 μl nuclease-free water and 1 μl SR RT Primer for Illumina were added to the ligation mixture, and the total volume was 25.5 μl. The samples were heated for 5 min at 75°C, 15 min at 37°C and 15 min at 25°C. Next, 1.1 μl 5′ SR adaptor was aliquoted into a separate nuclease-free 200 μl PCR tube. The adaptor was incubated in a thermal cycler at 70°C for 2 min, and then the tube was immediately placed on ice. The following components were added to the 3′ adaptor ligation mixture and mixed well: 1 μl 5′ SR adaptor, 1 μl 5′ ligation reaction buffer (10×) and 2.5 μl 5′ ligation enzyme mix. The mixture was

incubated for 1 h at 25°C in a thermal cycler. The 5′ adapter sequence was 5′-rGrUrUrCrArGrArGrUrUrC rUrArCrArGrUrCrCrGrArCrGrArUrC-3′. The 3′ adapter sequence was 5′-rAppAGATCGGAAGAGC ACACGTCT-NH2-3′. Then, reverse transcription and PCR amplification with adapter-specific primers were performed according to the protocol. Next, the 145–160 bp amplification products were isolated on a 6% polyacrylamide gel. Briefly, load wells with 25 µl of mixed Amplified cDNA Construct and loading dye on the 6% polyacrylamide gel. A total volume of 50 µl was loaded on the gel. The gel was run for 60 min at 145 V. Using a razor blade, the bands corresponding to adapter-ligated constructs derived from the 21 and 30 nucleotide RNA fragments, respectively, were cut out. Then, 300 µl ultra-pure water was added to the gel debris. The DNA was eluted by rotating or shaking the tube at room temperature for at least 2 h. The eluate and the gel debris were transferred to the top of a 5 µm filter. Then, 2 µl glycogen, 30 µl 3M NaOAc, 2 µl 0.1× pellet paint and 975 µl 100% pre-chilled ethanol (–25°C to –15°C) were added to the eluate. The eluate was immediately centrifuged at 20,000 g for 20 min at 4°C. The pellet was washed with 500 µl 70% ethanol at room temperature. Next, the pellet was re-suspended in 10 µl 10 mM Tris-HCl (pH 8.5). The concentration of each cDNA library was determined using a Qubit Fluorometer (Invitrogen), and samples were diluted for direct sequencing using the Illumina Hiseq2500 system (San Diego, CA) according to the manufacturer's protocol.

Basic data processing

The raw sequence reads produced by deep sequencing were pre-processed using the FASTX-Toolkit (http://hannonlab.cshl.edu/fastx_toolkit/). After adapter trimming, low-quality reads and reads shorter than 15 nt were removed to obtain clean reads. All clean reads were further annotated and classified by aligning to the pig genome mRAN (ftp://ftp.ensembl.org/pub/release-90/fasta/), miRBase (http://www.mirbase.org/), Rfam (http://rfam.xfam.org//) and RepBase (https://www.girinst.org/repbase/) databases. After alignment to Rfam and Genebank, non-miRNA reads (rRNA, tRNA, snoRNA and snRNA) were discarded, and the remaining reads (clean miRNA reads) were analysed by miRDeep2 (2.0.0.5) to identify known and novel miRNAs.[17]

MiRNA differential expression analysis

To determine miRNA differential expression between the LPS-stimulated and unstimulated groups, the expression of each miRNA was normalised to the total number of reads in the sample using the following formula: normalised expression = (actual miRNA read count/total clean read count) × 10^6.[18] The fold change in miRNA reads was presented as log 2 transformation using the following formula: fold change=log 2 (LPS/control).

Target prediction and functional analysis

The potential target genes of the differentially expressed miRNAs were predicted using MiRanda (http://www.microrna.org/microrna/getDownloads.do). We applied DAVID 6.8 to perform gene ontology (GO) functional classification and pathway enrichment analysis of the target genes.

Statistical analyses

The data are shown as means $\pm$ SD. Differences were tested using ANOVA and Student's paired t-test. The level of significance was set at $P < 0.05$ for all data analyses.

Results

The up-regulated expressions of TNF-α, IL-1β and IL-6 in LPS-stimulated PBMCs

In order to identify principal LPS-responsive miRNAs, PBMCs isolated from the whole blood of the three healthy pigs were stimulated with LPS for 8 h to induce inflammation. We applied ELISA to determine the protein levels of TNF-α and IL-1β. As shown in Figure 1a, the concentration of TNF-α and IL-1β in supernatants of the LPS-stimulated PBMCs were obviously increased compared to the control ($P < 0.05$). Also, the mRNA of TNF-α, IL-1β and IL-6 were significantly expressed in PMBCs after LPS stimulation (Figure 1b; $P < 0.001$). These results indicated that acute inflammation was induced by LPS in porcine PBMCs. Then, the RNA samples from LPS-stimulated and unstimulated (control) PMBCs were collected and used for further small RNA sequencing.

General analysis of small RNAs

Three independent RNA libraries were constructed for both the LPS-stimulated and unstimulated PBMCs, and then deep sequenced using the Illumina Hiseq2500 system. The six small RNA libraries from LPS treatment groups L1–L3 and control groups N1–N3 yielded a total of 30,002,256, 26,862,983, 25,945,596, 28,820,384, 25,815,123 and 22,992,993 raw reads, respectively. After eliminating adaptor and low-quality reads, a total of 25,785,759, 23,072,789, 21,888,402, 24,466,303, 21,924,186 and 19,793,933
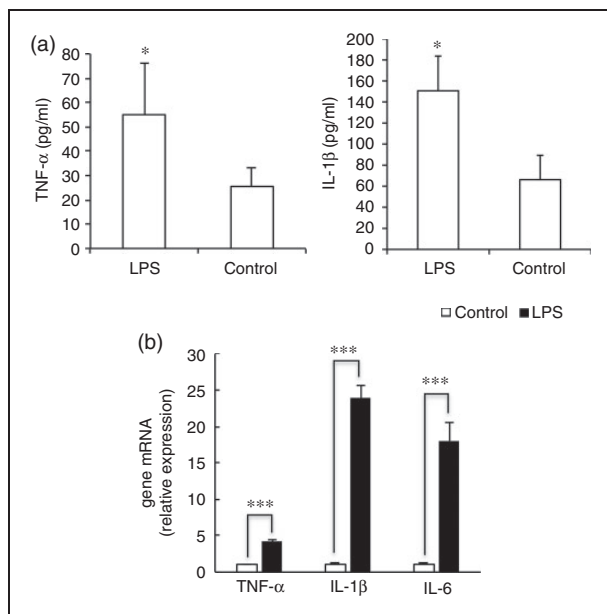
Figure 1. LPS-induced acute inflammation in porcine PBMCs. (a) The concentration of TNF-α in supernatants of the PBMCs were measured 8 h after treatment with or without LPS. (b) TNF-α, IL-1β and IL-6 mRNA expression were determined by quantitative PCR in porcine PBMCs 8 h after treatment with or without LPS. The data represent the mean ± SD. $n = 3$. *$P < 0.05$; ***$P < 0.001$.

clean reads were obtained in the L1–L3 and N1–N3 libraries, respectively (Table 1). All clean reads were then aligned to the pig genome databases (i.e. miRBase, Rfam, RepBase and mRNA/EST; Table 1). The sequence length distribution in the six libraries exhibited wide variation, ranging from 14 to 41 nt. Most of the small RNAs were 20–3 nt in length, predominantly 22 nt, which is the typical length of Dicer-derived products (Figure 2).

Identification of known and novel miRNAs

By performing BLASTN searches against miRBase v21.0, a total of 291 known miRNAs were identified (Supplemental Table S2). The relative number of normalised sequence reads of each miRNA was considered as an indication of its abundance. The top 10 most abundant miRNAs (ssc-miR-148a-3p, ssc-let-7g, ssc-let-7f, 3_8760, ssc-miR-26a, ssc-miR-451, ssc-miR-21, ssc-miR-30d, ssc-miR-99a and ssc-miR-103) in the two groups were ordered by the average proportion of each miRNA read relative to the total normalised miRNA reads (Figure 3). Then, we identified novel miRNAs in our small RNA deep-sequencing libraries by miRDeep2, which predicted 274 potential novel miRNAs at the relatively stringent score cut-off of 5 and signal-to-noise ratio of 17.1 (Table 2). The

Table 1. Preliminary analysis of high-throughput sequencing data.

Classes of reads	L1 library Total	L1 library Unique	L2 library Total	L2 library Unique	L3 library Total	L3 library Unique	N1 library Total	N1 library Unique	N2 library Total	N2 library Unique	N3 library Total	N3 library Unique
Clean date	25,785,759	1,882,643	23,072,789	1,507,672	21,888,402	1,763,266	24,466,303	1,900,191	21,924,186	1,453,039	19,793,933	1,265,303
Genome	24,235,018	1,326,766	21,851,349	1,069,799	20,665,172	1,294,325	23,108,678	1,389,212	20,755,282	1,045,953	19,135,840	1,010,364
miRBase (mature)	4,872,852	16,956	5,101,616	16,000	3,605,342	14,657	4,263,915	16,816	5,387,847	16,781	4,469,633	15,698
Rfam	1,133,522	38,240	918,263	32,297	878,052	34,177	1,107,982	40,942	1,003,033	33,014	953,020	30,332
RepBase	221,235	92,023	151,962	61,800	206,513	83,082	229,111	95,103	193,212	78,332	186,421	74,032
mRNA/EST	4,657,234	569,759	3,542,469	444,827	3,810,512	521,039	4,630,433	583,603	4,133,526	474,371	4,220,406	457,810

L1, L2 and L3 represent three experimental libraries (LPS-stimulated PBMCs); N1, N2 and N3 represent three control libraries (unstimulated PBMCs).
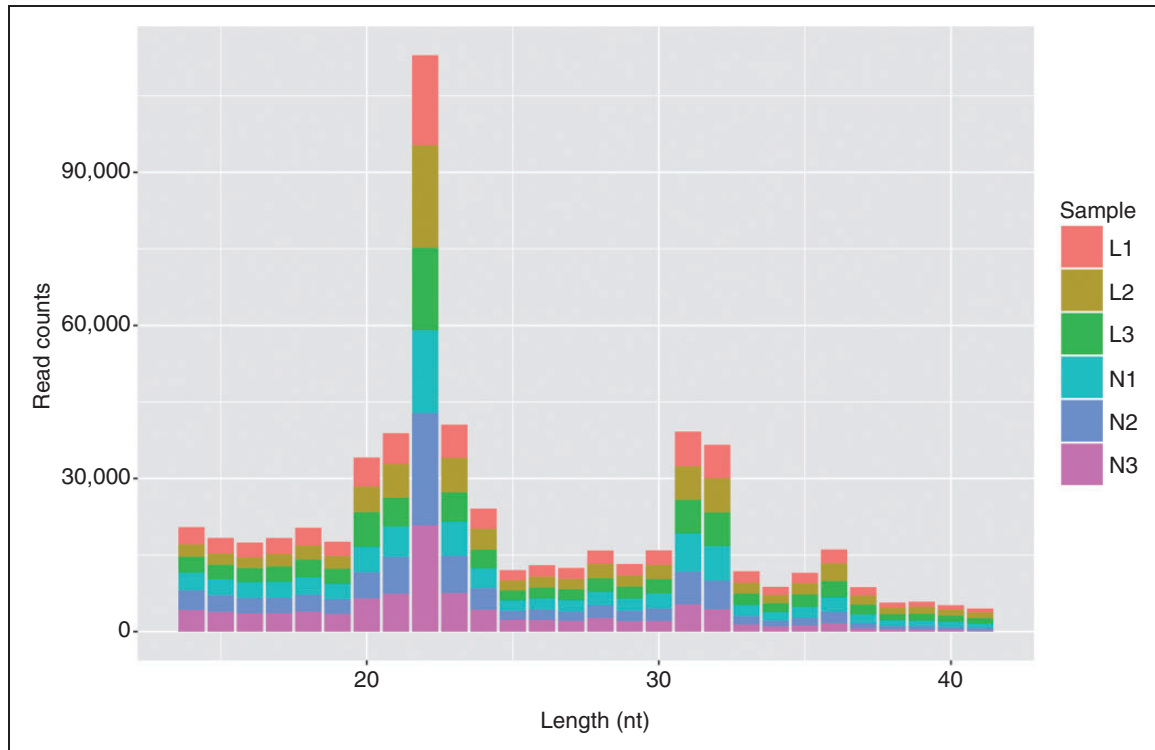
Figure 2. Length distribution of sequencing reads in the six libraries.
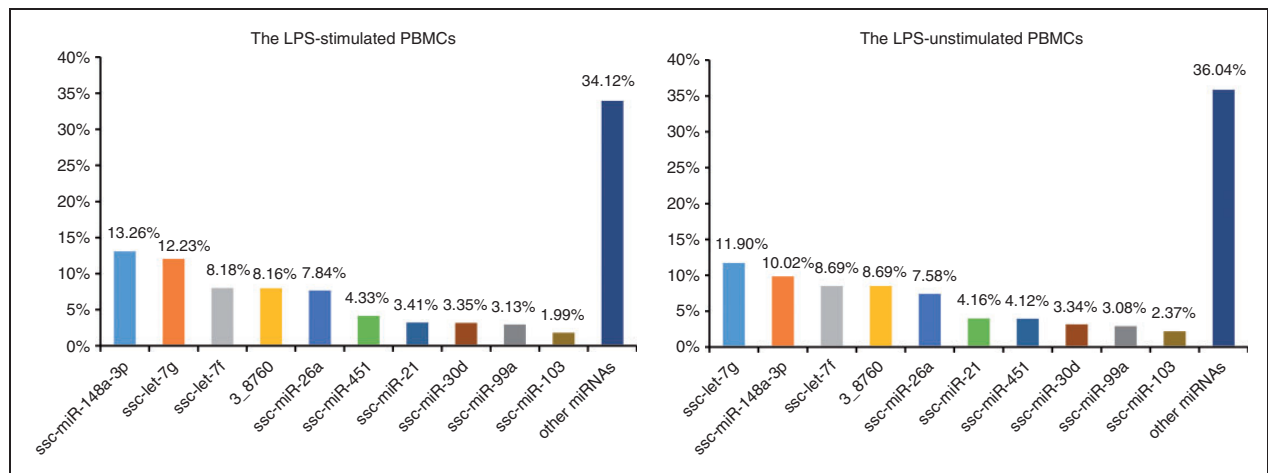
Figure 3. Top 10 most abundant miRNAs in the LPS-stimulated and unstimulated porcine PBMCs ordered by the average proportion of each miRNA read relative to total normalised miRNA reads.

predicted novel miRNAs were then filtered by removal of RNA without hairpin structure, which reduced the list to 228 novel miRNAs with significant randfold P-values ($P \leq 0.05$; Supplemental Table S3). Among these 228 new miRNAs, only eight miRNAs were sequenced more than 1×10^6 times, including 3_8760, 15_39442, 5_15093, 10_27878, 3_9803, 10_28549,

3_9801 and 13_3274 (Supplemental Table S3). Secondary structures for these eight candidates are shown in Figure 4.

Differential expression analysis

To investigate the changes in miRNA expression in porcine PBMCs after *in vitro* stimulation by LPS,

Table 2. Survey by miRDeep2 analysis showing the number of novel miRNAs under different score cut-offs ranging from 10 to 1.

| miRDeep2 score[a]	Predicted[b]	False-positives[c]	True-positives[d]	Signal-to-noise ratio[e]
10	160	14 ± 4	146 ± 4 (91 ± 2%)	18.8
9	167	14 ± 4	153 ± 4 (92 ± 2%)	18.8
8	175	15 ± 4	160 ± 4 (92 ± 2%)	18.7
7	183	15 ± 4	168 ± 4 (92 ± 2%)	18.5
6	191	17 ± 4	174 ± 4 (91 ± 2%)	17.7
5	274	23 ± 5	251 ± 5 (92 ± 2%)	17.1
4	307	53 ± 7	254 ± 7 (83 ± 2%)	8.5
3	321	153 ± 12	168 ± 12 (52 ± 4%)	3.2
2	435	207 ± 13	228 ± 13 (52 ± 3%)	2.9
1	713	284 ± 16	429 ± 16 (60 ± 2%)	3.1

[a]The miRDeep2 score represents the log-odds probability of a sequence being a genuine miRNA precursor versus the probability that it is a background hairpin, given the evidence from the data.
[b]Number of novel miRNA hairpins with a score greater than or equal to the cut-off.
[c]Number of false-positive miRNA hairpins predicted at this cut-off, as estimated by the miRDeep2 controls. Mean and standard deviation are estimated from 100 rounds of permuted controls.
[d]Number of true-positive miRNA hairpins is estimated as $t =$ total novel miRNAs–false-positive novel miRNAs. The percentage of the predicted novel miRNAs that are estimated to be true positives is calculated as $p = t$/total novel miRNAs. The number of false-positives is estimated from 100 rounds of permuted controls. In each of the 100 rounds, t and p are calculated, generating means and SD of t and p. The variable p can be used as an estimation of the miRDeep2 positive predictive value at the score cut-off.
[e]For the given score cut-off, the signal-to-noise ratio is estimated as $r =$ total miRNA hairpins reported/mean estimated false positive miRNA hairpins over 100 rounds of permuted controls.
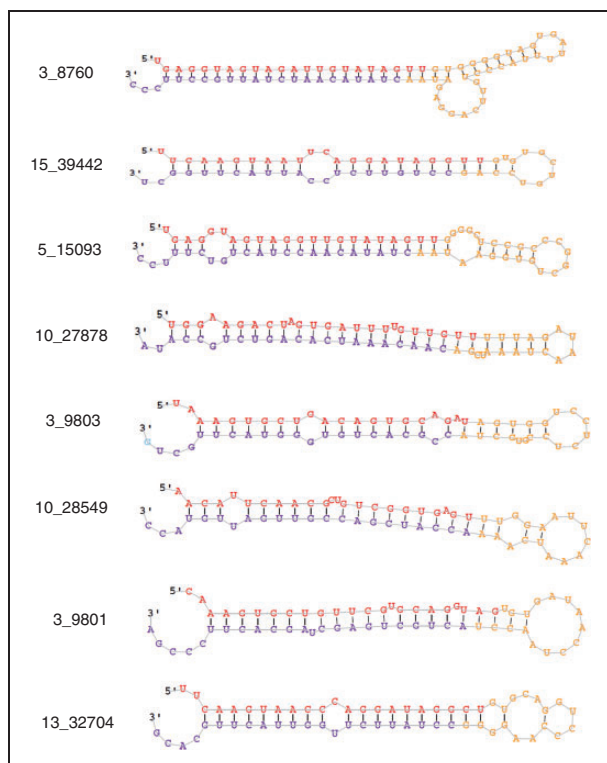
Figure 4. Predicted stem-loop secondary structures of eight candidate novel pig miRNAs. Red: mature sequence; purple: star sequence with no reads cover; yellow: stem sequence.

we analysed differential expression of miRNAs between the LPS-stimulated and unstimulated PBMCs. After normalisation of the raw reads, we found that six miRNAs (17_42478, ssc-miR-122, 5_14697_star, 2_6974, ssc-miR-129b and 15_39332) were significantly up-regulated in the LPS-stimulated PBMCs with a P value cut-off of 0.05. Similarly, nine miRNAs (ssc-miR-152, 4_12780, ssc-miR-17-5p, 8_24906, 3_9803, 15_40039, 6_17355, ssc-miR-144 and 1_3912) were significantly down-regulated (Table 3). Differential expressions of five selected miRNAs (ssc-miR-122, ssc-miR-129b, ssc-miR-152, ssc-miR-17-5p and ssc-miR-144) were validated by quantitative PCR. As shown in Figure 5, quantitative RT-PCR validated that ssc-miR-122 and ssc-miR-129b were significantly up-regulated by LPS, while ssc-miR-152 and ssc-miR-17-5p were down-regulated. However, ssc-miR-144 showed no obvious change in PBMCs after LPS stimulation.

GO and functional classification

The potential targets of the novel differentially expressed miRNAs are listed in Supplemental Table S4. The genes associated with the significantly enriched GO terms and KEGG pathways are shown in Figures 6 and 7, respectively. The GO annotation was classified

into three functional categories: 40 catalogues of biological process (BP), 16 catalogues of cellular component (CC) and seven catalogues of molecular function (MF). In the biological process category, most of the annotated targets were involved in the positive regulation of transcription from RNA polymerase II promoter, the negative regulation of cell proliferation and the intracellular protein transport. In the cellular component category, most targets were assigned to the cytoplasm and the extracellular exosome. In the molecular function category, most targets were associated with the thiol-dependent ubiquitin-specific protease activity, the cysteine-type endopeptidase activity and the protein heterodimerisation activity.

Furthermore, KEGG pathway analysis demonstrated that the target genes were mainly involved in immunity, such as the pathways in cancer, endocytosis, the chemokine signalling pathway, the TNF signalling pathway, the TLR signalling pathway and the T-cell receptor signalling pathway.

Discussion

As a potent agonist of TLR4, LPS can activate TLR4 signalling and induces the expression of the inflammatory cytokines TNF-α, IL-1β and IL-6.[4] In this study, LPS stimulated the production of TNF-α, IL-1β and IL-6 in porcine PBMCs, indicating that acute inflammation was induced by LPS challenge.

To our knowledge, this study is the first to survey miRNA expression profiles in porcine PBMCs with LPS stimulation. A total of 291 known miRNAs and 228 novel miRNAs were identified in our sequencing. Zhang et al. identified the miRNA signature of human blood mononuclear cells and found 108 highly expressed miRNAs.[19] We found that there were common miRNAs with abundance expressions in both human and porcine PBMCs, such as miR-148, let-7, miR-26, miR-21, miR-99, miR-30 and miR-103. Singh et al. used miRNA sequencing to explore the miRNA expression profiles in TLR ligand-stimulated and non-stimulated PBMCs isolated from the blood of healthy Murrah buffaloes. They found that the abundantly expressed miRNAs include bta-miR-103, bta-miR-19b, -191 -29b, -15a, -19a, -30d, -30b-5p and members of the let family (let 7a-5p, let 7g and let 7f) in LPS- and CpG-treated and control samples, while bta-miR-21-5p was highly expressed in LPS-treated PBMCs only.[20] In our sequencing libraries, four

Table 3. miRNAs significantly up- or down-regulated in LPS stimulated PBMCs.

| miRNAs ID	LPS_mean_TPM	Control_mean_TPM	Fold change-Log2
17_42478	1.8	0.1	4.2
ssc-miR-122	24.4	8.5	1.5
5_14697_star	7.8	2.9	1.4
2_6974	8.6	3.4	1.3
ssc-miR-129b	2.3	1.0	1.2
15_39332	310.2	205.9	0.6
ssc-miR-152	1176.1	1801.7	−0.6
4_12780	211.1	327.1	−0.6
ssc-miR-17-5p	2834.3	4499.5	−0.7
8_24906	795.9	1297.2	−0.7
3_9803	1743.8	2857.3	−0.7
15_40039	4	8.4	−1.1
6_17355	6.6	13.9	−1.1
ssc-miR-144	367.5	793.3	−1.1
1_3912	3.9	9.6	−1.3

Figure 5. Quantitative PCR was performed to verify expressions of the five miRNAs (ssc-miR-122, ssc-miR-129b, ssc-miR-152, ssc-miR-17-5p and ssc-miR-144) in RNA sequencing. Expression was normalised by U6. The data represent the mean $\pm$ SD. n $=$ 3. $*P < 0.05$; $**P < 0.01$.
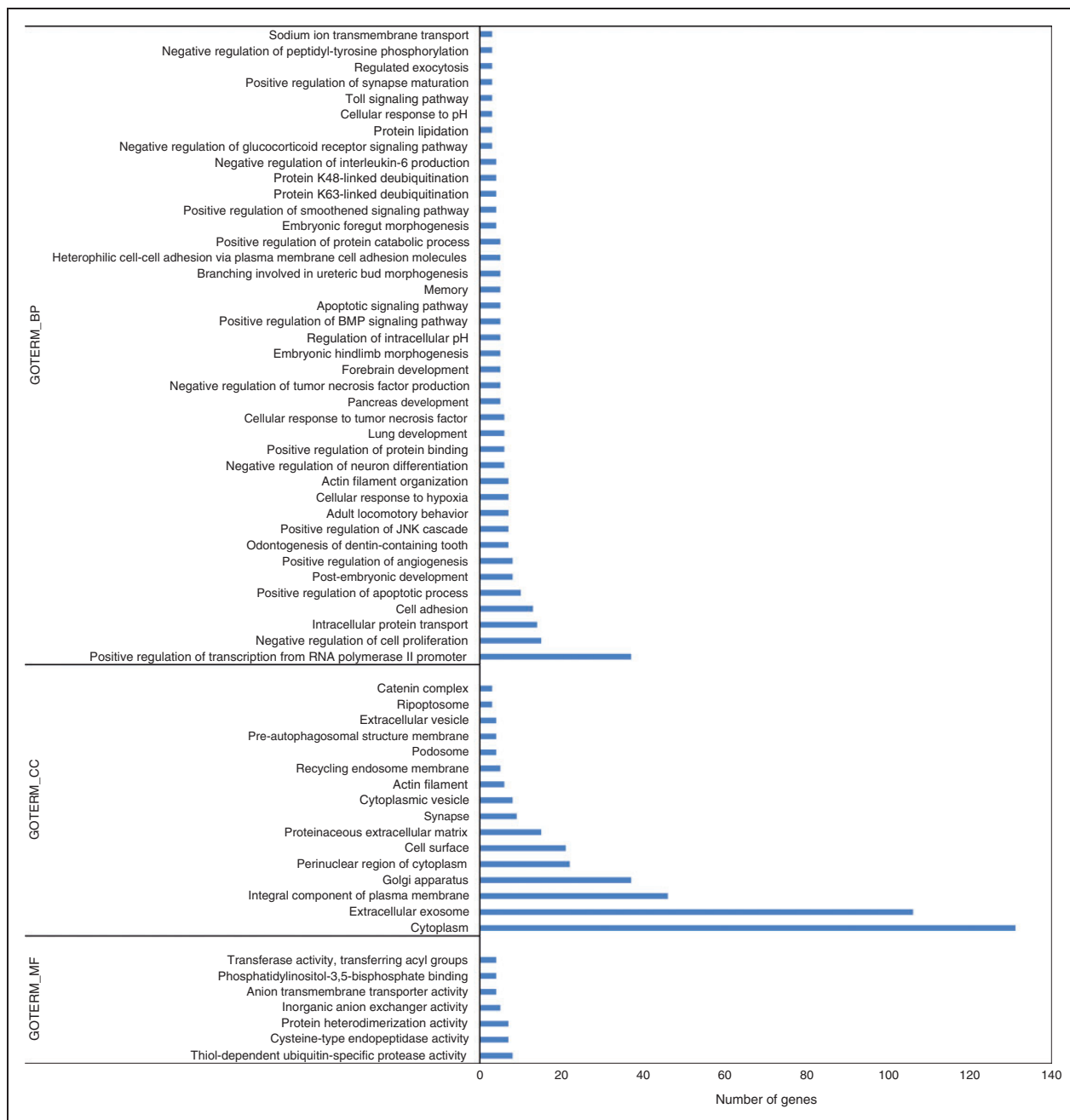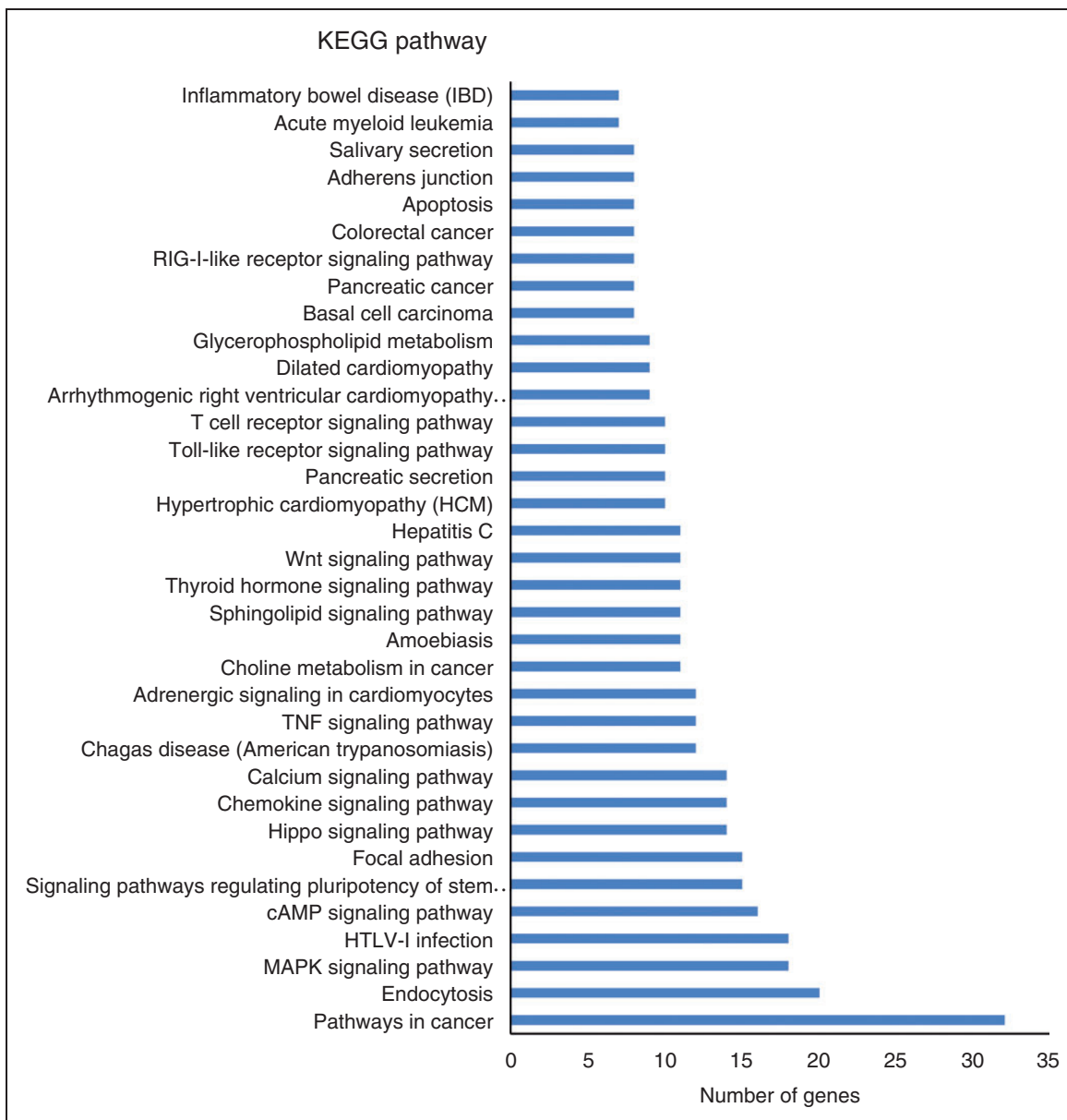
Figure 6. Gene ontology functional analysis of the potential targets of the novel differentially expressed miRNAs. We display the enriched pathway terms with a *P* value of < 0.05 according to DAVID v6.8.

miRNAs (ssc-let-7g, ssc-let-7f, ssc-miR-30d and ssc-miR-103) were also identified with high abundance, accounting for 26.78% and 26.30% of the total normalised miRNA reads in the LPS-treated and control groups, respectively. However, we found that ssc-miR-21 was abundantly expressed in both LPS-treated and control samples. The other most abundant miRNAs shared between the LPS-stimulated and unstimulated PBMCs were ssc-miR-148a-3p, 3_8760, ssc-miR-26a, ssc-miR-451 and ssc-miR-99a. We performed GO and KEGG analysis of the potential targets of the top nine most abundant known miRNAs (ssc-miR-148a-3p, ssc-let-7g, ssc-let-7f, 3_8760, ssc-miR-26a, ssc-miR-451, ssc-miR-21, ssc-miR-30d, ssc-miR-99a and ssc-miR-103). The results are shown in Supplemental Figures S1 and S2. In the biological process category, most of the annotated targets were involved in the regulation of transcription from RNA polymerase II promoter. In the cellular component category, most targets were assigned to the cytoplasm, nucleus and nucleoplasm.

KEGG pathway

Figure 7. KEGG pathway analysis of the potential targets of the novel differentially expressed miRNAs. We display the enriched pathway terms with a *P* value of < 0.05 according to DAVID v6.8.

In the molecular function category, most targets were associated with zinc ion binding and ATP binding. The KEGG pathways predictions indicated a significant enrichment in GO functional categories related to the phosphatidylinositol signalling system, HTLV-I infection and protein processing in the endoplasmic reticulum. MiR-148a is implicated in a series of biological processes, including cellular proliferation, apoptosis, metastasis and invasion.[21–23] MiR-26a has been reported to regulate important cellular processes such as cellular differentiation, cell growth, apoptosis and metastasis, thereby participating in the initiation and development of various diseases.[24] MiR-451 and

miR-99a play role in a variety of tumours and are potential candidates for therapy.[25–27] However, there is very little specific information on the expression and function of these four miRNA in PBMCs.

In the present study, four known miRNAs (ssc-miR-122, ssc-miR-129b, ssc-miR-152 and ssc-miR-17-5p) and 10 novel miRNAs showed expression changes on LPS stimulation of porcine PBMCs. MiR-122 is the most abundant miRNA in the liver, which can be involved in liver biology and disease.[28,29] It can directly target cyclin G1, Bcl-w (anti-apoptosis gene), WNT1 and so on.[30–32] A recent study reported that miR-122 plays a role in innate immunity by regulating TLR4

expression in hepatoma cells.[33] MiR-129 has been shown to be involved in the formation of many types of cancer and attenuates cell proliferation by targeting high-mobility group box 1 (HMGB1).[34,35] As a ubiquitous nuclear protein, HMGB1 acts as a danger signal when released extracellularly after cellular activation, stress, damage or death.[36] Extracellular HMGB1 is a mediator implicated in the pathogenesis of many inflammatory conditions and diseases.[37] Therefore, further studies have to be carried out in porcine PBMCs to identify the potential functions of ssc-miR-122 and ssc-miR-129b, and the target genes in inflammatory process. The ssc-miR-152 and ssc-miR-17-5p have more abundant expression in PBMCs compared to other differentially expressed miRNAs. Previous studies reported that MiR-152 can impair innate response by targeting calcium/calmodulin-dependent protein kinase II (CaMKIIα).[38,39] CaMKIIα, a major downstream effector of calcium (Ca^{2+}), could promote TLR-triggered production of pro-inflammatory cytokines and type I IFN.[40] MiR-17-5p is a well-known oncogenic miRNA, which regulates tumorigenesis, proliferation, invasiveness and cell-cycle progression by targeting various tumour suppressors.[41–43] A recent study by Ji et al. found that miR-17-5p expression significantly decreased in PBMCs isolated from mice which were injected with 50 mg/kg LPS for 4 h.[44] These data are consistent with our results. In addition, Ji et al. found that overexpression of miR-17-5p inhibited LPS-induced IL-1β and TNF-α expressions in macrophages (RAW264.7 cells) by targeting TLR4.[44] According to our miRNA sequencing data, ssc-miR-129b were poorly expressed (<10 TPM per miRNA) in porcine PBMCs, while the four miRNAs (ssc-miR-122, ssc-miR-152 and ssc-miR-17-5p) were modestly expressed (10–10,000 TPM per miRNA). Therefore, further studies must be carried out in porcine PBMCs to identify the potential functions and target genes of ssc-miR-122, ssc-miR-152 and ssc-miR-17-5p in inflammatory process. However, ssc-miR-129b existed at low levels and might have little impact on immunity or inflammation in porcine PBMCs.

In addition, we performed function analysis of the potential targets of the novel differentially expressed miRNAs. Target gene and KEGG pathway predictions indicated a significant enrichment in GO functional categories related to diseases, immunity and inflammation, including the pathways in cancer, endocytosis, MAPK signalling pathway, HTLV-I infection, the chemokine signalling pathway, the TNF signalling pathway, the TLR signalling pathway and the T-cell receptor signalling pathway. For example, we predicted that IL12RB1 was the potential target of the novel miRNA 17_42478. IL12RB1 is a Mendelian susceptibility to mycobacterial disease (MSMD) gene, which is essential for mycobacterial disease resistance and T-cell differentiation.[45] In addition, we predicted TRAF3 was the potential target of the novel miRNA 5_14697. In TLR and RIG-I-like receptor (RLR) signalling pathways, TRAF3 is a highly versatile regulator that positively controls type I IFN production but negatively regulates MAPK activation and alternative NF-κB signalling.[46] TRAF3 is also known to function as a resident nuclear protein, and to impact B-cell survival and activation.[47] CXCL2 (macrophage inflammatory protein-2 (MIP-2)), a critical chemokine for neutrophils, controls the early stage of neutrophil recruitment during inflammation.[48] TLR4-expressing tissue macrophages release CXCL2 following stimulation with LPS.[49] CEBPB is a transcription factor activated by LPS or IL-17, and itself regulates numerous genes involved in inflammation, including IL-6 and IL-23R.[50,51] We predicted CXCL2 and CEBPB were the potential targets of the novel miRNA 2_6974 and 6_17355, respectively.

Here, we have provided the changes of miRNA expression in LPS-stimulated PBMCs of pigs, which will serve as a reference point for future functional studies or challenge experiments directed to uncover the role of miRNAs in immunity and disease pathogenesis.

ORCID iD

Yulan Liu https://orcid.org/0000-0001-9617-9305

Supplemental material

Supplemental material for this article is available online.

References

1. McOrist S, Khampee K and Guo A. Modern pig farming in the People's Republic of China: growth and veterinary challenges. *Rev Sci Tech* 2011; 30: 961–968.

2. Yang H, Paruch L, Chen X, et al. Antibiotic application and resistance in swine production in China: current situation and future perspectives. *Front Vet Sci* 2019; 6: 136.

3. Camargo LN, Righetti RF, Aristóteles LRCR, et al. Effects of anti-IL-17 on inflammation, remodeling, and oxidative stress in an experimental model of asthma exacerbated by LPS. *Front Immunol* 2018; 8: 1835.

4. Lu YC, Yeh WC and Ohashi PS. LPS/TLR4 signal transduction pathway. *Cytokine* 2008; 42: 145–151.

5. Lai JL, Liu YH, Liu C, et al. Indirubin inhibits LPS-induced inflammation via TLR4 abrogation mediated by the NF-κB and MAPK signaling pathways. *Inflammation* 2017; 40: 1–12.

6. Tsutsui H, Imamura M, Fujimoto J, et al. The TLR4/TRIF-mediated activation of NLRP3 inflammasome underlies endotoxin-induced liver injury in mice. *Gastroenterol Res Pract* 2010; 2010: 1–11.

7. Roy S and Sen CK. miRNA in wound inflammation and angiogenesis. *Microcirculation* 2012; 19: 224–232.

8. Yan Y, Lu K, Ye T, et al. MicroRNA-223 attenuates LPS-induced inflammation in an acute lung injury model via the NLRP3 inflammasome and TLR4/NF-κB signaling pathway via RHOB. *Int J Mol Med* 2019; 43: 1467–1477.

9. Cao M, Zhang W, Li J, et al. Inhibition of SIRT1 by microRNA-9, the key point in process of LPS-induced severe inflammation. *Arch Biochem Biophys* 2019; 666: 148–155.

10. Park H, Huang X, Lu C, et al. MicroRNA-146a and microRNA-146b regulate human dendritic cell apoptosis and cytokine production by targeting TRAF6 and IRAK1 proteins. *J Biol Chem* 2015; 290: 2831–2841.

11. Zhang K, Song F, Lu X, et al. MicroRNA-322 inhibits inflammatory cytokine expression and promotes cell proliferation in LPS-stimulated murine macrophages by targeting NF-κB1 (p50). *Biosci Rep* 2017; 37: BSR20160239.

12. Tang B, Xuan L, Tang M, et al. MiR-93-3p alleviates lipopolysaccharide-induced inflammation and apoptosis in H9c2 cardiomyocytes by inhibiting toll-like receptor 4. *Pathol Res Pract* 2018; 214: 1686–1693.

13. Xie N, Cui H, Banerjee S, et al. MiR-27a regulates inflammatory response of macrophages by targeting IL-10. *J Immunol* 2014; 193: 327–334.

14. Tili E, Michaille JJ, Cimino A, et al. Modulation of miR-155 and miR-125b levels following lipopolysaccharide/TNF-α stimulation and their possible roles in regulating the response to endotoxin shock. *J Immunol* 2007; 179: 5082–5089.

15. Liu Y, Lu J, Shi J, et al. Increased expression of the peroxisome proliferator-activated receptor gamma in the immune system of weaned pigs after *Escherichia coli* lipopolysaccharide injection. *Vet Immunol Immunopathol* 2008; 124, 82–92.

16. Livak KJ and Schmittgen TD. Analysis of relative gene expression data using real-time quantitative PCR and the $2^{-\Delta\Delta CT}$ method. *Methods* 2001; 25: 402–408.

17. Dhahbi JM, Atamna H, Boffelli D, et al. Deep sequencing reveals novel microRNAs and regulation of microRNA expression during cell senescence. *PLoS One* 2011; 6: e20509.

18. Zhang J, Fu SL, Liu Y, et al. Analysis of MicroRNA expression profiles in weaned pig skeletal muscle after lipopolysaccharide challenge. *Int J Mol Sci* 2015; 16: 22438–22455.

19. Zhang Q, Cannavicci A, Dai SC, et al. MicroRNA signature of human blood mononuclear cells. *Mol Cell Biochem* 2019; 462: 167–172.

20. Singh J, Mukhopadhyay CS, Kaur S, et al. Identification of the microRNA repertoire in TLR-ligand challenged bubaline PBMCs as a model of bacterial and viral infection. *PLoS One* 2016; 11: e0156598.

21. Li Y, Deng X, Zeng X, et al. The role of miR-148a in cancer. *J Cancer* 2016; 7: 1232–1241.

22. Babu KR and Muckenthaler MU. MiR-148a regulates expression of the transferrin receptor 1 in hepatocellular carcinoma. *Sci Rep* 2019; 9: 1518.

23. Wang W, Dong J, Wang M, et al. miR-148a-3p suppresses epithelial ovarian cancer progression primarily by targeting c-Met. *Oncol Lett* 2018; 15: 6131–6136.

24. Li X, Pan X, Fu X, et al. MicroRNA-26a: an emerging regulator of renal biology and disease. *Kidney Blood Press Res* 2019; 44: 287–297.

25. Li L, Gao R, Yu Y, et al. Tumor suppressor activity of miR-451: identification of CARF as a new target. *Sci Rep* 2018; 8: 375.

26. Liu Y, Li B, Yang X, et al. MiR-99a-5p inhibits bladder cancer cell proliferation by directly targeting mammalian target of rapamycin and predicts patient survival. *J Cell Biochem* 2019; 120: 19330–19337.

27. Tsai TF, Lin JF, Chou KY, et al. miR-99a-5p acts as tumor suppressor via targeting to mTOR and enhances RAD001-induced apoptosis in human urinary bladder urothelial carcinoma cells. *Onco Targets Ther* 2018; 11: 239.

28. Barajas JM, Reyes R, Guerrero MJ, et al. The role of miR-122 in the dysregulation of glucose-6-phosphate dehydrogenase (G6PD) expression in hepatocellular cancer. *Sci Rep* 2018; 8: 9105.

29. Howell LS, Ireland L, Park BK, et al. MiR-122 and other microRNAs as potential circulating biomarkers of drug-induced liver injury. *Expert Rev Mol Diagn* 2018; 18: 47–54.

30. Gramantieri L, Ferracin M, Fornari F, et al. Cyclin G1 is a target of miR-122a, a microRNA frequently down-regulated in human hepatocellular carcinoma. *Cancer Res* 2007; 67:6092–6099.

31. Lin CJ, Gong HY, Tseng HC, et al. MiR-122 targets an anti-apoptotic gene, Bcl-w, in human hepatocellular carcinoma cell lines. *Biochem Biophys Res Commun* 2008; 375: 315–320.

32. Ahsani Z, Mohammadi-Yeganeh S, et al. WNT1 gene from WNT signaling pathway is a direct target of miR-122 in hepatocellular carcinoma. *Appl Biochem Biotechnol* 2017; 181: 884–897.

33. Shi L, Zheng X, Fan Y, et al. The contribution of miR-122 to the innate immunity by regulating toll-like receptor 4 in hepatoma cells. *BMC Gastroenterol* 2019; 19: 130.

34. Wang S, Chen Y, Yu X, et al. miR-129-5p attenuates cell proliferation and epithelial mesenchymal transition via HMGB1 in gastric cancer. *Pathol Res Pract* 2019; 215: 676–682.

35. Zheng L, Qi Y X, Liu S, et al. miR-129b suppresses cell proliferation in the human lung cancer cell lines A549 and H1299. *Genet Mol Res* 2016; 15.

36. Klune JR, Dhupar R, Cardinal J, et al. HMGB1: endogenous danger signaling. *Mol Med* 2008; 14: 476–484.

37. Andersson U, Yang H and Harris H. Extracellular HMGB1 as a therapeutic target in inflammatory diseases. *Expert Opin Ther Targets* 2018; 22: 263–277.

38. Wang Y, Tian Y, Ding Y, et al. MiR-152 may silence translation of CaMK II and induce spontaneous immune tolerance in mouse liver transplantation. *PLoS One* 2014; 9: e105096.

39. Liu X, Zhan Z, Xu L, et al. MicroRNA-148/152 impair innate response and antigen presentation of TLR-triggered dendritic cells by targeting CaMKIIα. *J Immunol* 2010; 185: 7244–7251.

40. Liu X, Yao M, Li N, et al. CaMKII promotes TLR-triggered proinflammatory cytokine and type I interferon production by directly binding and activating TAK1 and IRF3 in macrophages. *Blood* 2008; 112: 4961–4970.

41. Wu Q, Luo G, Yang Z, et al. miR-17-5p promotes proliferation by targeting SOCS6 in gastric cancer cells. *FEBS Lett* 2014; 588: 2055–2062.

42. Zhu Y, Gu J, Li Y, et al. MiR-17-5p enhances pancreatic cancer proliferation by altering cell cycle profiles via disruption of RBL2/E2F4-repressing complexes. *Cancer Lett* 2018; 412: 59–68.

43. Matsubara H, Takeuchi T, Nishikawa E, et al. Apoptosis induction by antisense oligonucleotides against miR-17-5p and miR-20a in lung cancers overexpressing miR-17-92. *Oncogene* 2007; 26: 6099.

44. Ji ZR, Xue WL and Zhang L. Schisandrin B Attenuates inflammation in LPS-induced sepsis through miR-17-5p downregulating TLR4. *Inflammation* 2019; 42: 731–739.

45. Reeme AE, Claeys TA, Aggarwal P, et al. Human IL12RB1 expression is allele-biased and produces a novel IL12 response regulator. *Genes Immun* 2019; 20: 181–197.

46. Häcker H, Tseng PH and Karin M. Expanding TRAF function: TRAF3 as a tri-faced immune regulator. *Nat Rev Immunol* 2011; 11: 457–468.

47. Bishop GA, Stunz LL and Hostager BS. TRAF3 as a multifaceted regulator of B lymphocyte survival and activation. *Front Immunol* 2018; 9: 2161.

48. Filippo D, Katia, Hogg, et al. Mast cell and macrophage chemokines CXCL1/CXCL2 control the early stage of neutrophil recruitment during tissue inflammation. *Blood* 2013;121: 4930–4937.

49. De Filippo K, Henderson RB, Laschinger M, et al. Neutrophil chemokines KC and macrophage-inflammatory protein-2 are newly synthesized by tissue macrophages using distinct TLR signaling pathways. *J Immunol* 2008; 180: 4308–4315.

50. Simpson-Abelson MR, Hernandez-Mir G, Childs EE, et al. CCAAT/Enhancer-binding protein b promotes pathogenesis of EAE. *Cytokine* 2017; 92: 24–32.

51. Roos AB, Barton JL, Miller-Larsson A, et al. Lung epithelial-C/EBPβ contributes to LPS-induced inflammation and its suppression by formoterol. *Biochem Biophys Res Commun* 2012; 423: 134–139.